

Progress in  
Physical Geography

**Vegetation structure influences the retention of airfall  
tephra in a sub-Arctic landscape**

Journal:	<i>Progress in Physical Geography</i>
Manuscript ID	PPG-15-094.R1
Manuscript Type:	Main Article
Keywords:	aeolian sediment, tephrochronology, Iceland, photogrammetric analysis, vegetation structure
Abstract:	<p>Vegetation cover mediates a number of important geomorphological processes. However, the effect of different vegetation types on the retention of fine aeolian sediment is poorly understood. We investigated this phenomenon, using the retention of fine, pyroclastic material (tephra) from the 2011 eruption of the Grímsvötn volcano, Iceland, as a case study. We set out to quantify structural variation in different vegetation types and to relate structural metrics to the thickness of recently deposited volcanic ash layers in the sedimentary section. We utilised a combination of vegetation and soil surveys, along with photogrammetric analysis of vegetation structure. We found that indices of plant community composition were a poor proxy for vegetation structure and were largely unrelated to tephra thickness. However, structural metrics, derived from photogrammetric analysis, were clearly related to variations in tephra layer thickness at a landscape scale and tephra layers under shrub patches were significantly thicker than those outside the shrub canopy. We therefore concluded that a) vegetation cover was a critical factor in the retention of fine aeolian sediment for deposit depths up to few centimetres and b) structural variation in vegetation cover played a major role in determining the configuration of tephra deposits in the sedimentary section. These findings have implications for the analysis of ancient volcanic eruptions and archaeological/palaeoenvironmental reconstructions based on the interpretation of tephra deposits. Furthermore, they present the possibility that the detailed form of tephra layers may be used as a proxy for palaeo vegetation structure.</p>

SCHOLARONE™  
Manuscripts

1  
2  
3  
4  
5  
6  
7  
8  
9     **1     Abstract**

10     2     Vegetation cover mediates a number of important geomorphological processes.  
11     3     However, the effect of different vegetation types on the retention of fine aeolian  
12     4     sediment is poorly understood. We investigated this phenomenon, using the retention  
13     5     of fine, pyroclastic material (tephra) from the 2011 eruption of the Grímsvötn volcano,  
14     6     Iceland, as a case study. We set out to quantify structural variation in different  
15     7     vegetation types and to relate structural metrics to the thickness of recently deposited  
16     8     volcanic ash layers in the sedimentary section. We utilised a combination of vegetation  
17     9     and soil surveys, along with photogrammetric analysis of vegetation structure. We  
18     10    found that indices of plant community composition were a poor proxy for vegetation  
19     11    structure and were largely unrelated to tephra thickness. However, structural metrics,  
20     12    derived from photogrammetric analysis, were clearly related to variations in tephra  
21     13    layer thickness at a landscape scale and tephra layers under shrub patches were  
22     14    significantly thicker than those outside the shrub canopy. We therefore concluded that  
23     15    a) vegetation cover was a critical factor in the retention of fine aeolian sediment for  
24     16    deposit depths up to few centimetres and b) structural variation in vegetation cover  
25     17    played a major role in determining the configuration of tephra deposits in the  
26     18    sedimentary section. These findings have implications for the analysis of ancient  
27     19    volcanic eruptions and archaeological/palaeoenvironmental reconstructions based on  
28     20    the interpretation of tephra deposits. Furthermore, they present the possibility that the  
29     21    detailed form of tephra layers may be used as a proxy for palaeo vegetation structure.  
30  
31  
32  
33  
34  
35  
36  
37  
38  
39  
40  
41  
42  
43

44     **24     Keywords**

45     25    Aeolian sediment, tephrochronology, Iceland, photogrammetric analysis, vegetation  
46     26    structure  
47  
48  
49  
50  
51  
52  
53  
54  
55  
56  
57  
58  
59  
60

1  
2  
3  
4  
5  
6  
7  
8 **28 Introduction**  
9

10 29

11 30 Vegetation cover is a key factor in terrestrial geomorphology, as it mediates  
12 31 microclimate, hydrological processes and mass movement (Marston, 2010). Vegetation  
13 32 plays a particularly important role in the entrapment and stabilisation of sediment  
14 33 carried by fluids, whether the fluid is water (e.g. salt marshes) or air (e.g. sand dunes)  
15 34 (see, e.g., Baas, 2002; Langlois et al., 2003). However, the precise impact of different  
16 35 vegetation types on terrestrial sediment cycles is still poorly understood. For example,  
17 36 volcanoes produce considerable quantities of airborne ash and this material is a major  
18 37 component of soils worldwide (Takahashi and Shoji, 2002). However, the processes by  
19 38 which fine, pyroclastic particles (tephra) are trapped and incorporated into soils are not  
20 39 well defined. In contrast to the quasi-continuous aeolian deposition typical of arid or  
21 40 coastal environments, tephra are typically deposited rapidly, ballistically and in discrete  
22 41 events (often separated by many years), so the rules that govern other forms of  
23 42 sediment accumulation may not be strictly applicable. Vegetation cover is likely to play  
24 43 a role in the retention of tephra, **but the importance of this factor** has not been explored.  
25 44 The overall aim of this research was therefore to investigate how different vegetation  
26 45 types influence the retention of episodically deposited aeolian sediment, using the  
27 46 deposition of volcanic ash as an exemplar.  
28 47  
29 48

30 49 Previous work has indicated that the capacity of vegetation to trap and retain sediment  
31 50 is dependent upon its structure (the physical configuration of above ground biomass  
32 51 and the intervening voids: Zehm et al., 2003) and the way in which this structure  
33 52 modifies local wind fields (**e.g. structural configurations which greatly reduce wind**  
34 53 **speeds are likely to result in sediment retention**). Many different metrics of vegetation  
35 54 structure have been proposed; however, previous studies have demonstrated that the  
36 55 ability of vegetation to trap sediment is **captured by** relatively straightforward  
37 56 characteristics e.g. vegetation height, density and porosity (**i.e. the network of voids**  
38  
39  
40  
41  
42  
43  
44  
45  
46  
47  
48  
49  
50  
51  
52  
53  
54  
55  
56  
57  
58  
59  
60

1  
2  
3  
4  
5  
6  
7  
8  
9 57 defined by stems, leaves, etc. within the vegetation: Moller, 2006). Whilst these  
10 58 aggregate characteristics are conceptually simple, they are difficult to measure reliably  
11 59 in the field. The most promising techniques for investigating vegetation structure have  
12 60 involved photogrammetry i.e. the quantitative analysis of high-resolution photographic  
13 61 images. Surveys utilising this technique have demonstrated that photogrammetric  
14 62 studies of vegetation can be rapid, detailed, reproducible and, under ideal  
15 63 circumstances, non-destructive (Moller, 2006; Neumeier, 2005; Zehm et al., 2003).  
16 64 Consequently, we set out to refine existing photogrammetric techniques in order to  
17 65 capture the essential structural characteristics of low-growing vegetation (mosses,  
18 66 forbs and short graminoids), structural types that have been neglected by previous  
19 67 researchers.  
20  
21  
22  
23  
24  
25  
26  
27

28 70 Our study focused on the deposition and retention of airfall tephra. Tephra particles are  
29 71 pyroclastic fragments produced during explosive volcanic eruptions (Lowe, 2011;  
30 72 Thorarinsson, 1944). Coarse tephra grains (lapilli with a diameter > ~4 mm) are rapidly  
31 73 sedimented from the atmosphere and are mostly confined to a region proximal to the  
32 74 volcano. However, fine grains may be transported considerable distances (100s to  
33 75 1000s km) in the atmosphere before they are deposited as airfall tephra (Stevenson et  
34 76 al., 2015). Once on the ground, they are readily mobilised by wind and water unless  
35 77 something acts to stabilise them (Sarna-Wojcicki et al., 1981). If the tephra deposit is  
36 78 stabilised and of sufficient thickness it can form clearly defined layers in sedimentary  
37 79 sections. These layers cover large parts of Earth's surface. Tephra deposits are of  
38 80 interest for three main reasons. Firstly, they may be used in the reconstruction of the  
39 81 fallout area and erupted volume of past volcanic eruptions (Lowe, 2011). When  
40 82 conducting reconstructions of this type, it is essential to know how faithfully the tephra  
41 83 layer records the characteristics of the initial deposit. This is particularly important in  
42 84 spatially extensive distal locations where the quantity of tephra is greatest (see, e.g.,  
43 85 Sarna-Wojcicki et al., 1981), but the deposit is thin, fine-grained and readily  
44  
45  
46  
47  
48  
49  
50  
51  
52  
53  
54  
55  
56  
57  
58  
59  
60

1  
2  
3  
4  
5  
6  
7  
8  
9 86 transformed. Secondly, tephra layers are frequently used as chronostratigraphic  
10 87 horizons (Lowe, 2011). In this case, all that matters is the identification of the isochron.  
11 88 Thirdly, if a tephra layer is considered to be a pulse of sediment of known age and  
12 89 provenance, it may be used as a tracer to understand a) geomorphological processes  
13 90 that are otherwise impractical to investigate e.g. aeolian erosion and deposition and b)  
14 91 the environmental impacts of an eruption, using palaeoecological techniques.  
15  
16  
17  
18  
19  
20  
21  
22  
23  
24  
25  
26  
27  
28  
29  
30  
31  
32  
33  
34  
35  
36  
37  
38  
39  
40  
41  
42  
43  
44  
45  
46  
47  
48  
49  
50  
51  
52  
53  
54  
55  
56  
57  
58  
59  
60

93  
94 The interpretation of tephra layers in the soil is premised on the assumption that the  
95 thickness of the layer in the soil is directly related to the thickness of the initial deposit.  
96 Airfall tephra mantles the landscape, i.e. the thickness of a fresh deposit is likely to be  
97 more-or-less the same in locations separated by a few kilometres, unless such  
98 locations are near the edge of the plume. However, tephra layers in the sedimentary  
99 section are often highly variable over small spatial scales (centimetres – metres)  
100 (Streeter and Dugmore, 2013b). If ancient tephra layers are to be correctly interpreted,  
101 it is necessary to understand the processes by which a fresh tephra deposit is  
102 ultimately transformed into a sedimentary layer. Thick tephra deposits (tens of cm –  
103 metres thick) obliterate vegetation cover and geomorphological processes are likely to  
104 determine the overall configuration of the final deposit. However, there is evidence that  
105 some vegetation can survive moderate (up to a few cms) tephra deposition. Some  
106 mosses, for example, are porous to fine tephra particles and can absorb light falls  
107 without detrimental effects. Bjarnason (1991) reported that carpets of the moss  
108 *Racomitrium lanuginosum* can absorb falls of up to 8cm without incurring significant  
109 damage; Zobel & Antos (1997) noted moss recovery from falls < 2cm in forest adjacent  
110 to Mount St. Helens and Hotes *et al* (2004) reported the recovery of *Sphagnum* spp.  
111 moss from beneath deposits 6cm thick. It is therefore possible that surviving biomass  
112 can trap and stabilise tephra, thus influencing the formation of tephra layers (Streeter  
113 and Dugmore, 2013a).  
114

1  
2  
3  
4  
5  
6  
7  
8  
9 115

10 116 A number of studies have investigated the impact of tephra deposition on vegetation  
11 117 cover (see, e.g., Kent et al., 2001; Arnalds, 2013a). However, few have considered the  
12 118 problem in reverse. This project investigated the relationship between vegetation  
13 119 structure and tephra depth on a series of sites in southern Iceland. Tephra-producing  
14 120 volcanic eruptions occur on average every 3 years in Iceland and the tephrochronology  
15 121 of the island is well constrained (Hafliðason et al., 2000; Thordarson and Larsen, 2007;  
16 122 Larsen et al., 1999). It is therefore an ideal location for a study of this type. Our specific  
17 123 research aims were to 1) assess the utility of plant community composition as a proxy  
18 124 for vegetation structure; 2) establish whether qualitatively different types of vegetation  
19 125 cover, defined largely on the basis of species composition, could be differentiated using  
20 126 photogrammetric analysis of structure and 3) relate metrics of vegetation structure to  
21 127 the thickness of recently deposited tephra layers in the sedimentary section.  
22  
23  
24  
25  
26  
27  
28  
29  
30

129

## 31 130 **Methods**

32 131

### 33 132 **Sampling locations**

34 133 The research was conducted on three sites in southern Iceland: Fossdalur, Kalfafell  
35 134 and Blómsturvellir (Fig. 1). The Kalfafell site provided two sampling locations (one  
36 135 dominated by moss and one by grass), giving four sampling locations in total (Table 1).  
37 136 Tephra were deposited on the sites during the 2011 eruption of the Grímsvötn volcano  
38 137 (hereafter referred to as G2011). The G2011 eruption produced ~0.6 – 0.8 km<sup>3</sup> of  
39 138 tephra which were subsequently distributed over a large area of southern Iceland  
40 139 (Gudmundsson et al., 2012). All of the study sites were located between 50-55 km from  
41 140 Grímsvötn caldera and within the main axis of fallout from the eruption (Fig. 1e). The  
42 141 initial depth of the tephra deposit was similar on all the sampling locations. By the time  
43 142 the surveys were conducted (June 2014) the G2011 tephra was not visible on the  
44 143 surface, either because the vegetation had grown through tephra and/or the particles  
45  
46  
47  
48  
49  
50  
51  
52  
53  
54  
55  
56  
57  
58  
59  
60

1  
2  
3  
4  
5  
6  
7  
8  
9 144 had percolated through the vegetation. Rather, the G2011 tephra formed a distinct,  
10 145 dark layer in the upper horizons of the soil. Three years of post-eruption deposition had  
11 146 led to a layer of sediment 0.25 – 1.5 mm thick on top of the tephra, deposition rates in  
12 147 line with measures of accumulation in southern Iceland over the past 100 years  
13 148 (Streeter and Dugmore, 2013a).  
14  
15  
16  
17  
18

19 151 The sampling locations were broadly flat or gently sloping and had limited  
20 152 microtopographic variation (Fig. 1). The key characteristic that varied between the  
21 153 sampling locations was vegetation cover, which was categorised qualitatively at the  
22 154 beginning of the study, based on the dominant functional type of vegetation. The major  
23 155 growth forms encountered were mosses, graminoids and dwarf shrubs. With the  
24 156 exception of the Blómsturvellir sampling location (where the moss/graminoid heath was  
25 157 interrupted by small shrub patches) we deliberately chose sampling locations with  
26 158 relatively homogeneous vegetation cover.  
27  
28  
29  
30  
31  
32

33 160 Table 1: Site characteristics  
34  
35

36 162 Fig. 1: Site photos  
37  
38  
39  
40

41 165 Vegetation surveys

42 166 The vegetation cover on each of the four sampling locations was recorded using  
43 167 systematic quadrat surveys (Table 1). A 50 x 50 cm quadrat was deployed on a grid;  
44 168 the grid dimensions varied according to the **size and shape** of each sampling location.  
45 169 We recorded all of the plant species present and estimated the cover of each taxon  
46 170 according to the Domin scale (Kent, 2012). The survey encompassed both mosses and  
47 171 vascular plants. The survey was conducted in June 2014; the 2011 tephra was  
48 172 deposited in March, so the vegetation at the time would have been relatively less  
49  
50  
51  
52  
53  
54  
55  
56  
57  
58  
59  
60

1  
2  
3  
4  
5  
6  
7  
8  
9 173 developed. However, the relative change in vegetation density between seasons is low  
10 174 in Iceland and we therefore assumed that the vegetation surveys would give us an  
11 175 indication of the relative differences between vegetation types.  
12  
13 176  
14  
15 177

16 178 The Blómsturvellir site, which was characterised by patches of woolly willow (*Salix*  
17 179 *lanata*) in a matrix of grass/moss heath, was initially surveyed using a grid of quadrats  
18 180 (the Bg survey). This survey mainly covered the low-growing vegetation (predominantly  
19 181 composed of mosses and graminoids). Ground-layer vegetation under the shrub  
20 182 patches was then surveyed using haphazardly-placed quadrats (the Bh survey, N =  
21 183 20), to see if the presence of a willow canopy impacted on the graminoid/bryophyte  
22 184 community.  
23  
24 185  
25 186  
26  
27 187

#### 28 188 Photogrammetric surveys

29 189 The survey technique applied was based on that developed by Zehm et al. (2003) and  
30 190 subsequently refined by others (Moller, 2006; Neumeier, 2005). A side-on, high-  
31 191 resolution digital photograph was taken of a patch of vegetation 35 cm across x 25 cm  
32 192 deep (Fig. 2). A 35 cm wide x 27 cm high white backing board was placed behind the  
33 193 target vegetation. The camera was positioned on a line normal to the centre of the  
34 194 board, at a distance of 80 cm. The vegetation immediately adjacent to the target zone  
35 195 was removed by excavation: this made the ground line visible and permitted high-  
36 196 resolution measurements of the underlying tephra layer. The remaining vegetation  
37 197 between the camera and the target zone was flattened with a board, so that it did not  
38 198 appear in the photograph.  
39  
40  
41  
42  
43  
44  
45  
46  
47

48 199 Fig. 2: cartoon of camera set-up  
49  
50  
51  
52  
53  
54  
55  
56  
57  
58  
59  
60



1  
2  
3  
4  
5  
6  
7  
8  
9 202 Tephra depth

10 203 The G2011 layer exposed in the excavated area was measured at five points at ~12.5  
11 204 cm intervals (i.e. at both ends of the exposed section and at three points in between).

12 205 The tephra layer was identified on the basis of colour (black, in contrast to the orange-  
13 206 brown andisol). Measurements of tephra thickness were made to the nearest  
14 207 millimetre.  
15  
16  
17  
18  
19

20 209  
21 210 Photographic image processing

22 211 The raw digital images were converted to grayscale and cropped to the boundaries of  
23 212 the backing board, using the programme Adobe Photoshop™. Each image was then  
24 213 processed using a bespoke routine written in MATLAB. First, the grayscale images  
25 214 were converted to black and white images using a threshold parameter that was  
26 215 adjusted according to camera exposure and vegetation type to ensure correspondence  
27 216 between pixel colour and true plant presence/absence. Starting from the base of each  
28 217 image and working upwards, the routine counted the numbers of black pixels  
29 218 (vegetation) in each row of the image, thereby encapsulating the vertical structure of  
30 219 the vegetation. From these data, it was straightforward to calculate the overall density  
31 220 of the vegetation i.e. the proportion of black pixels and the maximum height of the  
32 221 vegetation. However, these simple metrics are likely miss some of the complexity of the  
33 222 vegetation structure e.g., where maximum height is driven by a single, slender leaf that  
34 223 extends above the bulk of the vegetation. Consequently, the programme was designed  
35 224 to return more detailed structural metrics. For example, vegetation density (proportion  
36 225 of black pixels) at any given height may be calculated. It is also possible to derive more  
37 226 nuanced metrics of vertical vegetation structure e.g. the height below which a given  
38 227 proportion of black pixels occur ( $P_x$ , where  $x$  is proportion of the total number of pixels).  
39 228 If  $P_x$  is plotted against height, vegetation cover with different structural configurations  
40 229 would be expected to produce qualitatively different curves (Fig. 3).  
41  
42  
43  
44  
45  
46  
47  
48  
49  
50  
51  
52  
53  
54  
55  
56  
57  
58  
59  
60

1  
2  
3  
4  
5  
6  
7  
8  
9 231 Figs 3: Hypothetical analyses of vegetation structure

10 232

11 233

12  
13 234 Analysis

14 235 Detrended correspondence analysis (DCA) was applied to the vegetation survey data.

15 236 DCA is a robust multivariate technique that is capable of dealing with noisy data (ter

16 237 Braak, 1995). DCA was used to graphically represent the different vegetation

17 238 communities and to establish whether a) the initial, qualitative assessments of

18 239 vegetation type were supported by quantitative analysis of community composition and

19 240 b) how similar the ground layer vegetation under the willow canopy on the

20 241 Blómsturvellir site was to the surrounding, unshaded vegetation. DCA was also used to

21 242 calculate the compositional variability of the plant communities, expressed in terms of

22 243 multivariate inertia, a unitless metric of variability that is analogous to variance. If

23 244 community composition is a good proxy for vegetation structure and vegetation

24 245 structure influences tephra depth, then compositional variability should be correlated

25 246 with variation in the tephra thickness. Shannon diversity was also calculated as a

26 247 metric of compositional variability.

27 248

28 249

29 250 Photogrammetry was used to describe vegetation structure at each sampling location.

30 251 The MATLAB routine was used to calculate the cumulative proportion of black pixels

31 252 (P) with height for each quadrat. The distributions were then modelled for each

32 253 sampling location by fitting a curve of the form  $y = a(1 - e^{-bx})$ , which represents a

33 254 gradual attenuation of vegetation density with height (Fig. 3). This two-parameter

34 255 function was chosen as it provides sound fits and also contains parameters which are

35 256 intuitively helpful: a rate ( $b$ ) describing the change in density with height, and an

36 257 asymptote ( $a$ ) describing the total vegetation density of the image (i.e. the curvature of

37 258 the fitted line). The significance of the fit was established using Monte Carlo

38 259 techniques.

1  
2  
3  
4  
5  
6  
7  
8  
9 260  
10 261  
11 262 Mean tephra thicknesses on each site were analysed using ANOVA and the sites  
12 263 compared using a post hoc test (Tukey's HSD). We also calculated the coefficient of  
13 264 variation (CV) of tephra layer thickness for each sampling location, so this figure could  
14 265 be compared with variability in plant community composition. We assessed the  
15 266 relationship between vegetation structure and tephra thickness using a linear mixed  
16 267 effects model, with mean G2011 thickness in each quadrat as the response variable,  
17 268 vegetation height (derived from the photogrammetric analysis) as the fixed effect and  
18 269 site identity as the random effect. The variables were log-transformed prior to the  
19 270 analysis, which was conducted using the lme4 package in R (Bates et al., 2015). The  
20 271 significance of the model was assessed by comparing it to a null model (i.e. omitting  
21 272 the fixed effect) using ANOVA (Bolker et al., 2009).  
22 273

23  
24  
25  
26  
27  
28  
29  
30 274 We assumed that the extant plant community was a good analogue for vegetation  
31 275 cover at the time of the eruption as a) the initial tephra deposits were thin (previous  
32 276 work has estimated the critical deposit thickness for abrupt vegetation change in  
33 277 Iceland at 20 cm: Arnalds, 2013b) and b) Icelandic vegetation is very resilient and  
34 278 previous observations have shown how thin tephra deposits may percolate through the  
35 279 ground layer without disrupting plant growth (Bjarnason, 1991). The sampling locations  
36 280 were close to cultivated areas, but were not artificially cleared of G2011 tephra. The  
37 281 sites were visited by the authors immediately after the 2011 eruption, and annually  
38 282 thereafter: there was no evidence that vegetation had changed markedly post-G2011.  
39 283

40  
41  
42  
43  
44  
45 284

## 46 285 **Results**

47  
48 286  
49  
50  
51  
52  
53  
54  
55  
56  
57  
58  
59  
60

1  
2  
3  
4  
5  
6  
7  
8  
9 287 Vegetation surveys

10 288 The distribution of the quadrats in ordination space broadly matched the qualitative  
11 289 assessments of vegetation type. Quadrats on the left hand side of the DCA biplot (Fig.  
12 290 4a) could be characterised as grass-dominated vegetation (note the position of  
13 291 common grasses *Festuca* sp. and *Agrostis* sp. in relation to the quadrats from Kg and  
14 292 B). Those on the right hand side were moss-dominated: all the dominant moss species  
15 293 (*Racomitrium lanuginosum*, *R. ericoides*, *Hylocomium splendens*) were on this side,  
16 294 with the exception of *Rhytidiadelphus squarrosus*, a common moss often found in  
17 295 grass sward. The Fossdalur quadrats spanned both regions.  
18  
19  
20  
21  
22  
23  
24

25 296  
26 297  
27 298 The DCA also indicated that the sampling locations differed in terms of their  
28 299 compositional variability (Fig. 4a). The F and Km sites were the most variable in terms  
29 300 of community composition, based on the distribution of quadrats in ordination space  
30 301 and multivariate inertia (Table 2). In contrast, the Kg and B sites were tightly clustered  
31 302 and largely overlapping. On the Blómsturvellir site, there appeared to be no **substantial**  
32 303 difference between the vegetation under the willow canopy and the plant communities  
33 304 between the willow patches (Fig. 4b).  
34  
35  
36

37 305

38 306 Fig. 4: DCA biplot

39 307

40 308 Table 2: Metrics of variability

41 309

42 310 Models of vegetation structure

43 311 The exponential curve selected was a good fit for the data (Fig. 5): adjusted  $R^2$  values  
44 312 were all above 0.95, and the model parameters were highly significant in all cases ( $p <$   
45 313 0.001). The initial part of the fitted curve was clearly steeper on the mossy sites (F and  
46 314 Km). On the grassy sites (Kg and B), the curve was flatter (note the lower values of  $b$ :  
47  
48  
49  
50  
51  
52  
53  
54  
55  
56  
57  
58  
59  
60

1  
2  
3  
4  
5  
6  
7  
8  
9 315 Fig. 5). Mean vegetation height, represented in this case by the height below which  
10 316 70% of vegetation occurred (U0.7) was markedly higher on the grassy sites.

11 317

12  
13 318 Fig. 5: modelled curves for each sampling location

14 319

15 320

16  
17 321 Vegetation structure and tephra depth

18 322 Mean tephra depth varied significantly according to site location (ANOVA:  $F_{4,61} = 42.1$ ,

19 323  $p < 0.001$ ), even though the initial deposit depth was similar (Olsson et al., 2013). The

20 324 tephra layer in the Bh survey (i.e. under the willow canopy) was significantly thicker

21 325 than the G2011 layers in the other surveys; conversely, the layer on the Km site was

22 326 significantly thinner (Fig. 6). There was no significant difference in the thickness of the

23 327 tephra layers on the F, Kg and Bg sites.

24 328

25 329

26 330 U0.7 figures were used to express vegetation height in each quadrat. Maximum

27 331 vegetation height (U1.0) could have been used, but this figure is sensitive to the

28 332 presence of isolated stems and may be unrepresentative of overall vegetation

29 333 structure. At the scale of each sampling location, the relationship between vegetation

30 334 height and tephra thickness was unclear. However, at a landscape scale, tephra

31 335 thickness increased with vegetation height in a broadly hyperbolic fashion (Fig. 7). A

32 336 linear mixed effects model of the log-transformed data indicated a significant positive

33 337 relationship ( $\chi^2(1) = 8.46$ ,  $p = 0.004$ ).

34 338

35 339 Fig. 6: Box plots indicating G2011 tephra thickness in each sampling location.

36 340

37 341 Fig. 7: The relationship between vegetation height (U0.7) and G2011 thickness on the

38 342 sites.

39 343

40  
41  
42  
43  
44  
45  
46  
47  
48  
49  
50  
51  
52  
53  
54  
55  
56  
57  
58  
59  
60

344

345 **Discussion**

346

## 347 Vegetation composition

348 The results of the DCA were consistent with the qualitative assessments of vegetation  
349 types that were made during site selection. The sampling locations could be broadly  
350 divided into 'mossy' locations (Km) and 'grassy' locations (Kg, B), with Fossdalur  
351 occupying an intermediate position. The mossy sites were more variable, in terms of  
352 species composition and abundance, than the grassy sites. The apparent variability of  
353 the Km site was largely driven by the inclusion of a handful of quadrats that  
354 encompassed very different surface cover (i.e. two quadrats on totally eroded surfaces  
355 and several on boggy ground, located in the upper right quarter of Fig. 4a). When these  
356 quadrats were excluded, the Km location was less variable. Even allowing for this site-  
357 specific factor, a thick grass sward is likely to exclude colonisation by other plants and  
358 the hence suppress botanical diversity, so it was not unsurprising that the grassy sites  
359 were less variable.

360

361

362 If plant communities do influence tephra layer thickness, then one could hypothesise  
363 that variability in the plant community would be related to variability in the thickness of  
364 the G2011 tephra layer. Following from this, we had hoped that plant community  
365 composition would be a surrogate for vegetation structure. However, the relationship  
366 between community variability (Shannon diversity, multivariate inertia) and variability in  
367 the G2011 tephra layer was weak. Whilst plant community composition and vegetation  
368 structure are related on a fundamental level, within-species variation in growth form is  
369 likely to obscure this relationship. Furthermore, many species present in the plant  
370 community will make minimal contributions to the structural factors relevant for tephra  
371 stabilisation, whilst other species will dominate. For example, a single shrub species  
372 drove major changes in tephra depth on the Blómsturvellir site. **It is possible that plant**

1  
2  
3  
4  
5  
6  
7  
8  
9 373 traits related to structural features might be more useful predictors than species identity  
10 374 and this topic could be the focus of a future study. Without this information, the generic  
11 375 structural properties identified by the photogrammetric surveys appear to be much  
12 376 more informative than metrics of plant community composition.  
13  
14  
15  
16  
17  
18  
19  
20  
21  
22  
23  
24  
25  
26  
27  
28  
29  
30  
31  
32  
33  
34  
35

36  
37  
38  
39  
40  
41  
42  
43  
44  
45  
46  
47  
48  
49  
50  
51  
52  
53  
54  
55  
56  
57  
58  
59  
60

377  
378  
379 Ultimately, the relationship between plant community composition and tephra thickness  
380 will depend on the spatial scale at which the wind responds to variation in vegetation  
381 form. For example, the scale of turbulence in the wind is large compared to individual  
382 plants, then a relationship between plant community composition and tephra thickness  
383 would not necessarily be expected. Put another way, small-scale, plant-to-plant  
384 variation might not have any effect on the deposition or stabilisation of tephra. If this  
385 model applies, then the most meaningful vegetation data to collect would relate to  
386 structural properties averaged over a certain distance. We speculate that the key  
387 distance is larger than our quadrat size, but smaller than the quadrat spacing. Further  
388 spatial analysis based on transect measurements will be required to establish this.  
389  
390

391 Differentiating sampling locations on the basis of structural characteristics  
392 The models of vegetation structure derived from the photogrammetry captured  
393 qualitative differences between the sampling locations. On the Km site (dominated by a  
394 dense layer of the pleurocarpous moss, *R. lanuginosum*), the vegetation was clearly  
395 concentrated close to the ground. On sites dominated by graminoids, tall, erect stems  
396 meant that the vegetation was more evenly distributed over a range of heights,  
397 approximating the straight line plot in Fig. 3 (indicated by the lower values of  $b$  on the  
398 grassy sites). It was therefore possible to distinguish between the sampling locations in  
399 a physically meaningful way without explicitly referring to species identity. This finding  
400 has implications for the generalisation of our results to other locations.  
401

1  
2  
3  
4  
5  
6  
7  
8  
9 402

10 403 Survey methods other than photogrammetry could have been applied. For example, a  
11 404 pin-touch technique could have been used for conducting high-resolution surveys of  
12 405 vegetation height. However, this technique is relatively slow to apply in the field and  
13 406 records just one variable. In contrast, we found the photogrammetric approach to be  
14 407 relatively quick and the resulting data set rich and versatile.  
15  
16  
17  
18 408

19 409

20 410 Vegetation structure and tephra thickness

21 411 Our study strongly suggested that vegetation structure is a key factor in determining  
22 412 the thickness of the tephra layer preserved in the sedimentary section. This relationship  
23 413 is strongest at a landscape scale, i.e. between sampling locations. The relationship  
24 414 was less clear within sites (10s of m). At a site scale, variability in vegetation structure  
25 415 was limited as we chose sites with relatively homogeneous cover and noise (generated  
26 416 by unmeasured or essentially random processes) most likely obscured clear  
27 417 relationships. Higher resolution sampling of the vegetation may resolve this issue, as  
28 418 there was a mismatch between the scale of the vegetation metric (quadrat scale) and  
29 419 the tephra measurements (sub-quadrat scale).  
30  
31  
32  
33  
34  
35

36 420

37 421

38  
39 422 At a larger scale, where the variation in vegetation structure was greater, a positive  
40 423 correlation suggestive of a deterministic relationship emerged. This was probably  
41 424 because the large scale analyses included vegetation types at different ends of the  
42 425 continuum of vegetation types (moss vs tall grass and, in the case of Bh, dwarf  
43 426 shrubs). The relationship appeared to be non-linear. No G2011 tephra was observed  
44 427 on sites without vegetation cover i.e. the eroded sites within the Km sampling location.  
45 428 Presumably, fresh tephra on these denuded surfaces is readily eroded. When  
46 429 vegetation cover was low, small increases in vegetation height appeared to have a  
47 430 major impact on the thickness of tephra in the soil. In taller vegetation, height increases  
48  
49  
50  
51  
52  
53  
54  
55  
56  
57  
58  
59  
60



1  
2  
3  
4  
5  
6  
7  
8  
9 431 of the same magnitude have a smaller (but still broadly positive) effect, leading to  
10 432 hyperbolic relationship (Fig. 7). The analysis of tephra thickness on the Blómsturvellir  
11 433 site reinforced the impression that vegetation cover plays a major role in determining  
12 434 tephra depth. The tephra layers in patches of *Salix lanata* were significantly thicker  
13 435 than those under the surrounding, low-growing vegetation (Fig. 6), even though the  
14 436 plants in the ground layer were essentially the same.  
15  
16  
17  
18 437

19 438 This study focussed on aboveground vegetation structure as the major agent mediating  
20 439 tephra layer thickness. However, other factors also likely to be significant. Antecedent  
21 440 moisture levels, for example, are likely to change the 'stickiness' of newly deposited  
22 441 tephra. Plant traits that influence the way that moisture is retained on leaves and stems  
23 442 could therefore work alongside the morphological aspects of vegetation cover.  
24 443 Belowground structure might also be significant e.g. the particularly dense root  
25 444 structures associated with tussocky graminoids could influence the incorporation of  
26 445 tephra into the soil (although we did not observe this effect during our study).  
27  
28  
29  
30  
31  
32  
33  
34  
35  
36  
37  
38  
39  
40  
41  
42  
43  
44  
45  
46  
47  
48  
49  
50  
51  
52  
53  
54  
55  
56  
57  
58  
59  
60

#### 448 Implications of research

449 Our findings have clear implications for the interpretation of tephra layers. For the  
450 purposes of volcanic reconstruction, it is usually assumed that airfall tephra deposits do  
451 not undergo modification, unless they are very thick, in which case slope processes  
452 may come into play. However, our research shows that vegetation cover is likely to be  
453 important, too, particularly on smaller spatial scales and where the initial deposit depth  
454 is not so great that plant cover is extirpated. This finding offers the tantalising possibility  
455 that, under certain circumstances, variability in tephra layer thickness across a site may  
456 be used as a proxy for the vegetation cover extant at the time of the eruption (in terms  
457 of structure, if not taxonomy). This finding is especially important for the calculation of  
458 past eruptive volumes if vegetation cover may have varied significantly through time. If  
459 vegetation was significantly taller at the time of eruption, calculations of eruption

1  
2  
3  
4  
5  
6  
7  
8  
9 460 volume may be over-estimated. Furthermore, assessing variation in multiple, well-  
10 461 dated tephra layers may give insight into the spatio-temporal dynamics of vegetation  
11 462 cover over long time periods (Streeter and Dugmore, 2013a).  
12  
13 463  
14 464

15 465 **Conclusions**

16 466 Our research shows that the thickness of a recent tephra layer was correlated with the  
17 467 vegetation structure present at the time of deposition. We found that plant community  
18 468 composition was a poor surrogate for the physical structure of vegetation cover.  
19 469 However, photogrammetric analysis proved to be an effective way of capturing relevant  
20 470 structural characteristics. Analyses using this technique demonstrated that vegetation  
21 471 cover on different sites could be differentiated according to generic structural  
22 472 properties. These findings have implications for the interpretation of tephra layers,  
23 473 whether this work involves the analysis of ancient volcanic eruptions or  
24 474 archaeological/palaeoenvironmental reconstructions. Furthermore, it is possible that  
25 475 small-scale variability in tephra layers, rather than being interpreted as unhelpful  
26 476 'noise', could be used as a proxy for palaeo vegetation structure.  
27  
28  
29  
30  
31  
32  
33  
34  
35  
36  
37  
38  
39  
40  
41  
42  
43  
44  
45  
46  
47  
48  
49  
50  
51  
52  
53  
54  
55  
56  
57  
58  
59  
60

478 **References**

- 479 Arnalds O. (2013a) The Influence of Volcanic Tephra (Ash) on Ecosystems. In: Sparks  
 480 DL (ed) *Advances in Agronomy, Vol 121*. 331-380.
- 481 Arnalds O. (2013b) The Influence of Volcanic Tephra (Ash) on Ecosystems. In: Sparks  
 482 DL (ed) *Advances in Agronomy, Vol 121*. 331-380.
- 483 Baas ACW. (2002) Chaos, fractals and self-organization in coastal geomorphology:  
 484 simulating dune landscapes in vegetated environments. *Geomorphology* 48:  
 485 309-328.
- 486 Bates D, Maechler M, Bolker B, et al. (2015) Fitting linear mixed-effects models using  
 487 lme4. *Journal of Statistical Software* 67: 1-48.
- 488 Bjarnason ÁH. (1991) *Vegetation on lava fields in the Hekla area, Iceland*, Uppsala:  
 489 Acta Phytogeographica Suecica.
- 490 Bolker BM, Brooks ME, Clark CJ, et al. (2009) Generalized linear mixed models: a  
 491 practical guide for ecology and evolution. *Trends in Ecology & Evolution* 24:  
 492 127-135.
- 493 Gudmundsson MT, Höskuldsson Á, Larsen G, et al. (2012) The May 2011 eruption of  
 494 Grímsvötn. *EGU General Assembly*. Vienna, Austria: Copernicus.
- 495 Hafliðason H, Eiriksson J and Van Kreveld S. (2000) The tephrochronology of Iceland  
 496 and the North Atlantic region during the Middle and Late Quaternary: a review.  
 497 *Journal of Quaternary Science* 15: 3-22.
- 498 Hotes S, Poschod P, Takahashi H, et al. (2004) Effects of tephra deposition on mire  
 499 vegetation: a field experiment in Hokkaido, Japan. *Journal of Ecology* 92: 624-  
 500 634.
- 501 Kent M. (2012) *Vegetation description and data analysis*, Chichester: Wiley-Blackwell.
- 502 Kent M, Owen NW, Dale P, et al. (2001) Studies of vegetation burial: a focus for  
 503 biogeography and biogeomorphology? *Progress in Physical Geography* 25: 455  
 504 - 482.
- 505 Langlois E, Bonis A and Bouzille JB. (2003) Sediment and plant dynamics in  
 506 saltmarshes pioneer zone: *Puccinellia maritima* as a key species? *Estuarine*  
 507 *Coastal and Shelf Science* 56: 239-249.
- 508 Larsen G, Dugmore A and Newton A. (1999) Geochemistry of historical-age silicic  
 509 tephros in Iceland. *Holocene* 9: 463-471.
- 510 Lowe DJ. (2011) Tephrochronology and its application: A review. *Quaternary*  
 511 *Geochronology* 6: 107-153.
- 512 Marston RA. (2010) Geomorphology and vegetation on hillslopes: Interactions,  
 513 dependencies, and feedback loops. *Geomorphology* 116: 206-217.
- 514 Moller I. (2006) Quantifying saltmarsh vegetation and its effect on wave height  
 515 dissipation: Results from a UK East coast saltmarsh. *Estuarine Coastal and*  
 516 *Shelf Science* 69: 337-351.
- 517 Neumeier U. (2005) Quantification of vertical density variations of salt-marsh  
 518 vegetation. *Estuarine Coastal and Shelf Science* 63: 489-496.

- 1  
2  
3  
4  
5  
6  
7  
8  
9 519 Olsson J, Stipp SLS, Dalby KN, et al. (2013) Rapid release of metal salts and nutrients  
10 520 from the 2011 Grímsvötn, Iceland volcanic ash. *Geochimica et Cosmochimica*  
11 521 *Acta* 123: 134-149.
- 12 522 Sarna-Wojcicki AM, Shipley S, Waitt RB, et al. (1981) Areal Distribution, Thickness,  
13 523 Mass, Volume, and Grain Size of Air-Fall Ash from the Six Major Eruptions of  
14 524 1980. In: Lipman PW and Mullineaux DR (eds) *The 1980 Eruptions of Mount St.*  
15 525 *Helens, Washington*. Washington D.C.: USGS, 577-600.
- 16 526 Stevenson JA, Millington SC, Beckett FM, et al. (2015) Big grains go far: understanding  
17 527 the discrepancy between tephrochronology and satellite infrared measurements  
18 528 of volcanic ash. *Atmospheric Measurement Techniques* 8: 2069-2091.
- 19 529 Streeter R and Dugmore AJ. (2013a) Anticipating land surface change. *Proceedings of*  
20 530 *the National Academy of Sciences of the United States of America* 110: 5779-  
21 531 5784.
- 22 532 Streeter RT and Dugmore AJ. (2013b) Reconstructing late-Holocene environmental  
23 533 change in Iceland using high-resolution tephrochronology. *Holocene* 23: 197-  
24 534 207.
- 25 535 Takahashi T and Shoji S. (2002) Distribution and classification of volcanic ash soils.  
26 536 *Global Environmental Research* 6: 83-98.
- 27 537 ter Braak CJF. (1995) Ordination. In: Jongman RHG, ter Braak CJF and van Tongeren  
28 538 OFR (eds) *Data Analysis in Community and Landscape Ecology*. Cambridge:  
29 539 Cambridge University Press, 91-173.
- 30 540 Thorarinsson S. (1944) Tefrokronologiska studier på Island. *Geografiska Annaler* 26: 1-  
31 541 217.
- 32 542 Thordarson T and Larsen G. (2007) Volcanism in Iceland in historical time: Volcano  
33 543 types, eruption styles and eruptive history. *Journal of Geodynamics* 43: 118-  
34 544 152.
- 35 545 Zehm A, Nobis M and Schwabe A. (2003) Multiparameter analysis of vertical  
36 546 vegetation structure based on digital image processing. *Flora* 198: 142-160.  
37 547  
38 548  
39 549  
40  
41  
42  
43  
44  
45  
46  
47  
48  
49  
50  
51  
52  
53  
54  
55  
56  
57  
58  
59  
60

1  
2  
3  
4  
5  
6  
7  
8  
9 550 **Figure captions**

10 551

11 552 Fig. 1: The sampling locations: a) Fossdalur (F); b) the mossy Kalfafell sampling  
12 location (Km); c) the grassy Kalfafell sampling location (Kg) and d) Blómsturvellir (B:  
13 553 the lighter patches in the image are the dwarf willow, *Salix lanata*); e) the survey area.  
14  
15 554  
16 555

17 556 Fig. 2: Diagram indicating the set up used for the photogrammetric survey.  
18  
19 557

20 558 Fig. 3: Hypothetical analyses of different vegetation types (designated X, Y and Z). The  
21 559 vertical lines in the top three plots are diagrammatic representations of stems, viewed  
22 side-on; the height scale is indicative. The graph at the bottom of the image plots the  
23 560 proportion of biomass against height for each vegetation type. Hypothetical vegetation  
24 561 comprising vertical stems of equal height (vegetation type X) produces a straight line  
25 562 on the plot. Structural configurations where the vegetation thins with height (types Y  
26 563 and Z) produce plots of different curvatures.  
27  
28 564  
29 565

30 566 Fig. 4: DCA biplots, with each coloured circle indicating a quadrat survey. Plot a) is of  
31 567 all the sampling locations where grid surveys were conducted. The quadrats on the left  
32 568 hand side are broadly 'grassy' in terms of dominant growth form; those on the left are  
33 569 'mossy'. Plot b) illustrates the plant community on the Blómsturvellir site in more detail,  
34 570 comparing the grid survey (solid circles) with the haphazard survey of ground  
35 571 vegetation under willows (open circles). Key to common species: Agr\_sp = *Agrostis*  
36 572 species; Car\_sp = *Carex* sp.; Equ\_pal = *Equisetum palustre*; Fes\_sp = *Festuca*  
37 573 species; Hyl\_spl = *Hylocomium splendens*; Rac\_eri = *Racomitrium ericoides*; Rac\_lan  
38 574 = *Racomitrium lanuginosum*; Rhy\_squ = *Rhytidiadelphus squarrosus*.  
39  
40 575

41 576 Fig 5: Vertical vegetation structure for each sampling location. The points have been  
42 577 fitted with a curve of the form  $y = a(1 - e^{-bx})$ . In this case, the value of  $a$  (the  
43 578 asymptote) has been fixed at 1. The top two graphs (F, Km) have moss-dominated  
44  
45  
46  
47  
48  
49  
50  
51  
52  
53  
54  
55  
56  
57  
58  
59  
60

1  
2  
3  
4  
5  
6  
7  
8  
9 579 vegetation; those on the bottom have predominantly grassy vegetation cover. The  
10 580 mean height below which 70% of vegetation structure occurs (U0.7) is indicated on  
11 581 each plot.

12 582  
13 583 Fig. 6: Box plots showing mean tephra thickness in each sampling location. The  
14 584 thickness from the Bh survey (beneath willow canopy) is included for comparison.

15 585  
16 586 Fig. 7: The relationship between vegetation height (expressed here as U0.7, or the  
17 587 height below which 70% of vegetation occurs) and the mean thickness of the G2011  
18 588 tephra layer in each quadrat. Mean values  $\pm 1$  SE are indicated for each site. Key to  
19 589 sites: Km = Kalfafell (moss-dominated); F = Fossdalur (moss/grass heath); Kg =  
20 590 Kalfafell (grass-dominated); Bg = Blomsturvellir (grass/shrub).

21 591  
22  
23  
24  
25  
26  
27  
28  
29  
30  
31  
32  
33  
34  
35  
36  
37  
38  
39  
40  
41  
42  
43  
44  
45  
46  
47  
48  
49  
50  
51  
52  
53  
54  
55  
56  
57  
58  
59  
60

1

Site	Location	Survey area	No. quadrats	Vegetation cover
Fossdalur (F)	63.97° N 17.49° W, 75 m asl	30 x 30 m	36 at 6 m intervals	Moss heath dominated by <i>Racomitrium</i> spp. & <i>Hylocomium splendens</i> ; sparse graminoid cover (mainly <i>Agrostis</i> sp., <i>Kobresia myosuroides</i> ).
Kalfafell (moss) (Km)	63.97° N 17.65° W, 185 m asl	35 x 20 m	40 at 5 m intervals	Mainly low-diversity <i>Racomitrium lanuginosum</i> moss heath, but encompassing small, denuded areas and boggy patches.
Kalfafell (grass) (Kg)	63.96° N 17.66° W, 136 m asl	35 x 10 m	24 at 5 m intervals	Dense grass sward dominated by <i>Agrostis</i> sp.
Blómsturvellir (B)	63.97° N 17.65° W, 96 m asl	30 x 18 m	24 at 6 m intervals	Boggy ground characterised by mixture of grass (primarily <i>Festuca</i> sp., <i>Carex</i> spp.) and moss ( <i>Hylocomium splendens</i> , <i>Rhytidiadelphus squarrosus</i> ) heath with patches of <i>Salix lanata</i> .

2

3 Table 1: Details of sampling locations.

1  
2  
3  
4  
5  
6  
7  
8  
9  
10  
11  
12  
13  
14  
15  
16  
17  
18  
19  
20  
21  
22  
23  
24  
25  
26  
27  
28  
29  
30  
31  
32  
33  
34  
35  
36  
37  
38  
39  
40  
41  
42  
43  
44  
45  
46  
47  
48  
49  
50  
51  
52  
53  
54  
55  
56  
57  
58  
59  
60

1

Site	Shannon diversity, <i>H</i>	Multivariate inertia	CV of G2011
Fossdalur	1.23 ± 0.46	2.37	0.22
Kalfafell (moss)	0.64 ± 0.44	2.08	0.37
Kalfafell (grass)	1.44 ± 0.21	0.52	0.19
Blómsturvellir (grid)	1.59 ± 0.27	1.70	0.25

2

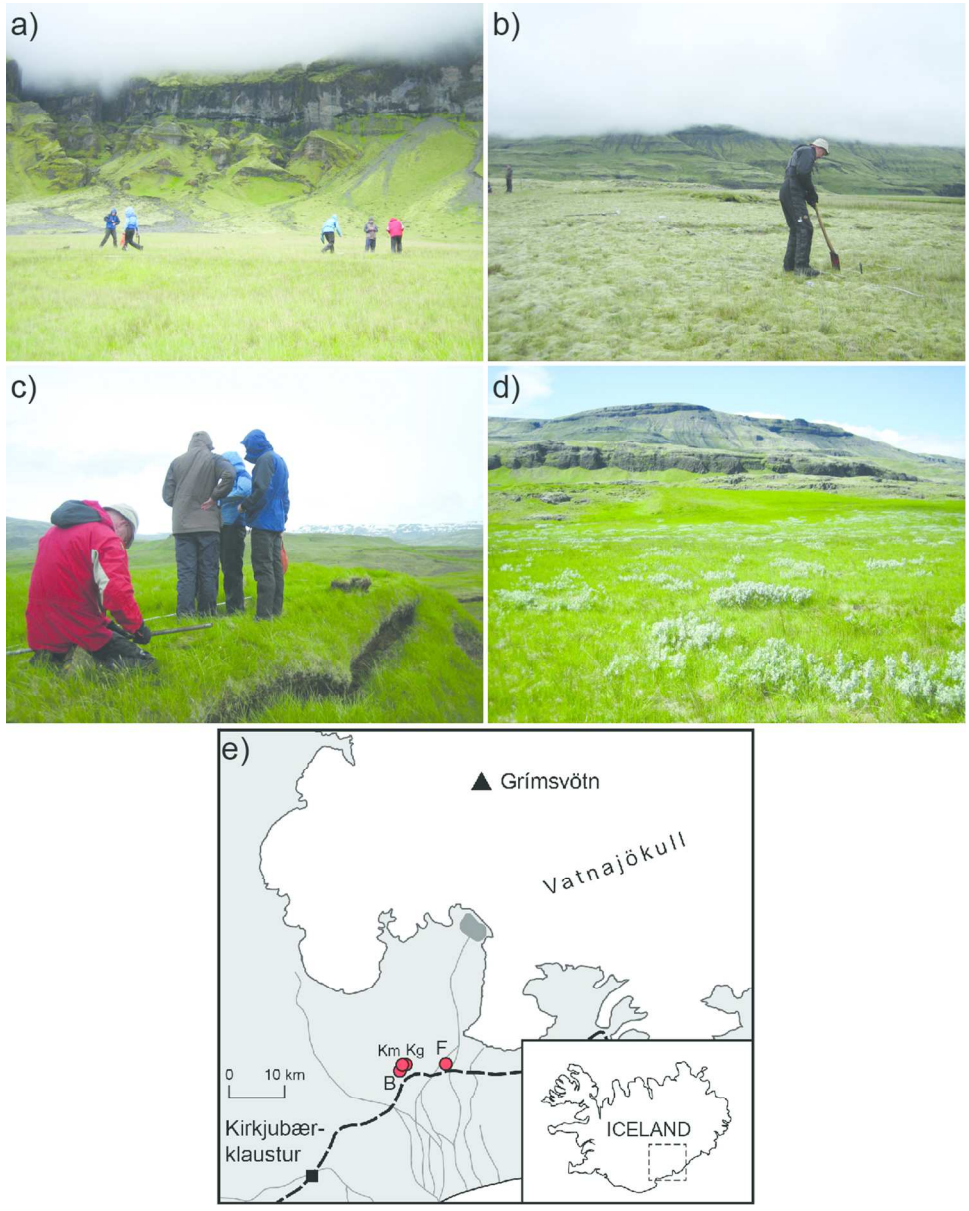
3 Table 2: Metrics of plant community diversity and variability in tephra layer depth (CV =  
4 coefficient of variation). Refer to Fig. 6 for mean tephra depths on each site.

5

Peer Review

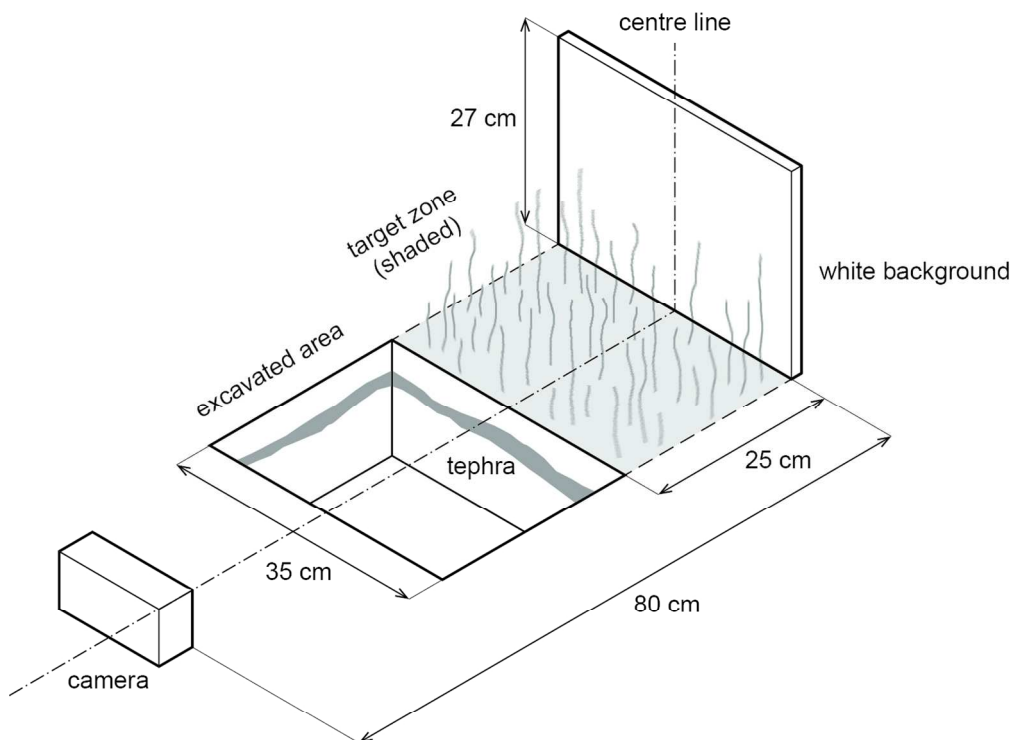


1  
2  
3  
4  
5  
6  
7  
8  
9  
10  
11  
12  
13  
14  
15  
16  
17  
18  
19  
20  
21  
22  
23  
24  
25  
26  
27  
28  
29  
30  
31  
32  
33  
34  
35  
36  
37  
38  
39  
40  
41  
42  
43  
44  
45  
46  
47  
48  
49  
50  
51  
52  
53  
54  
55  
56  
57  
58  
59  
60



107x134mm (300 x 300 DPI)

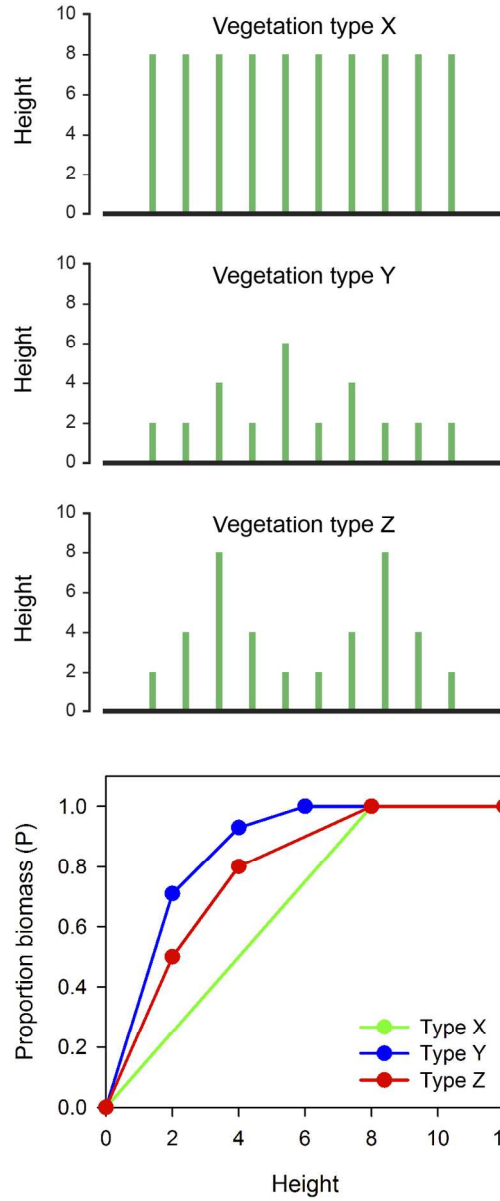
1  
2  
3  
4  
5  
6  
7  
8  
9  
10  
11  
12  
13  
14  
15  
16  
17  
18  
19  
20  
21  
22  
23  
24  
25  
26  
27  
28  
29  
30  
31  
32  
33  
34  
35  
36  
37  
38  
39  
40  
41  
42  
43  
44  
45  
46  
47  
48  
49  
50  
51  
52  
53  
54  
55  
56  
57  
58  
59  
60



130x106mm (300 x 300 DPI)

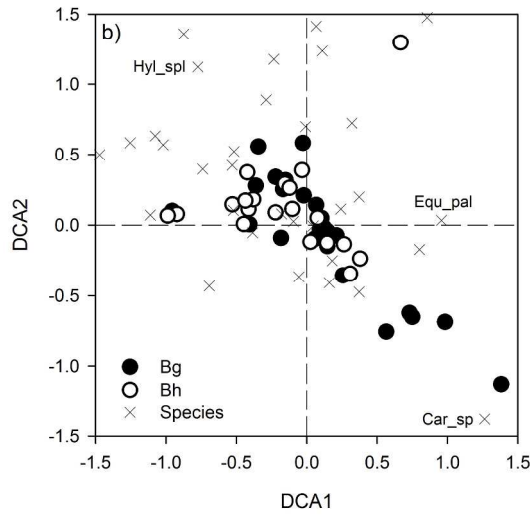
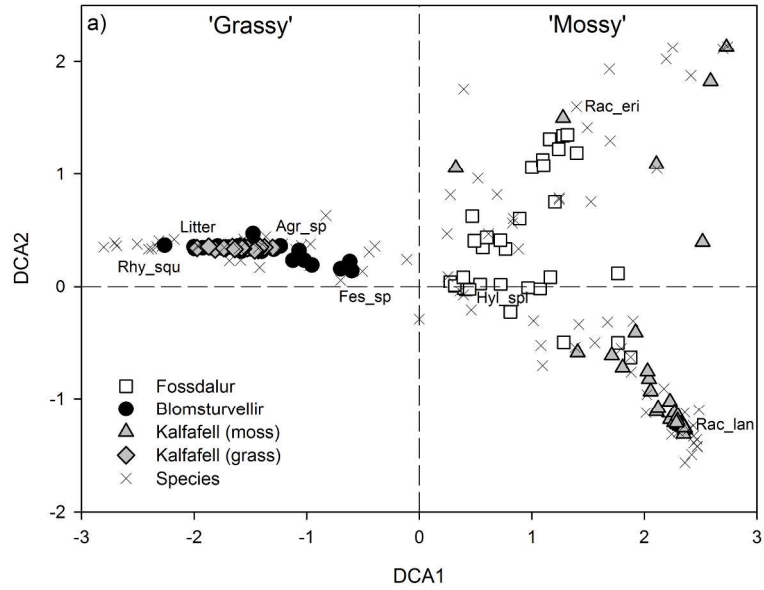
Review

1  
2  
3  
4  
5  
6  
7  
8  
9  
10  
11  
12  
13  
14  
15  
16  
17  
18  
19  
20  
21  
22  
23  
24  
25  
26  
27  
28  
29  
30  
31  
32  
33  
34  
35  
36  
37  
38  
39  
40  
41  
42  
43  
44  
45  
46  
47  
48  
49  
50  
51  
52  
53  
54  
55  
56  
57  
58  
59  
60

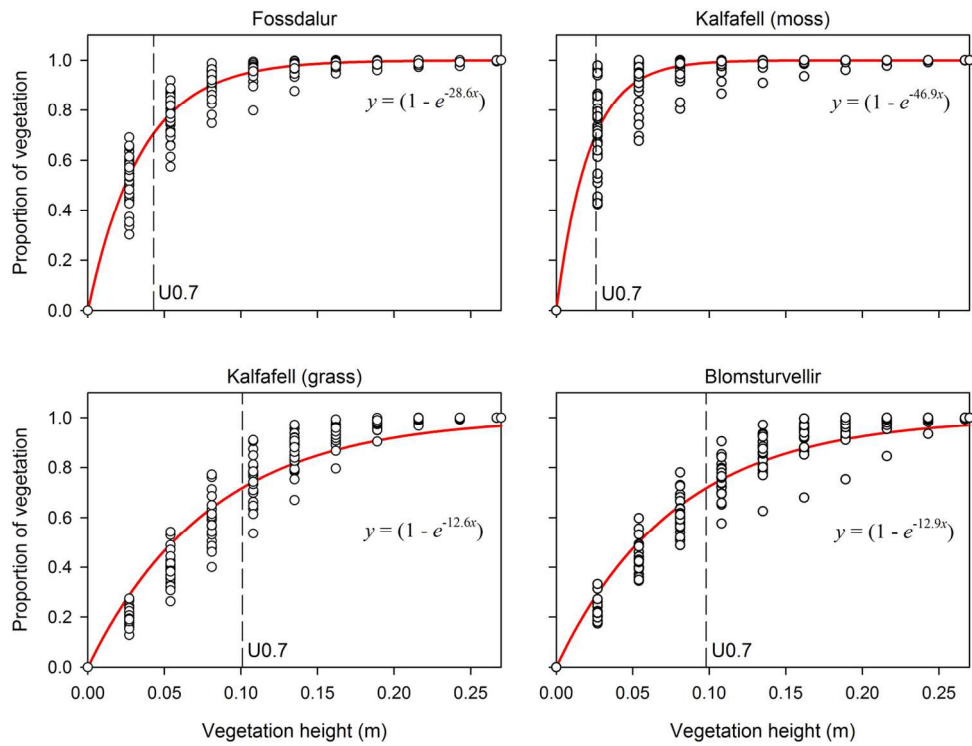


82x180mm (300 x 300 DPI)

1  
2  
3  
4  
5  
6  
7  
8  
9  
10  
11  
12  
13  
14  
15  
16  
17  
18  
19  
20  
21  
22  
23  
24  
25  
26  
27  
28  
29  
30  
31  
32  
33  
34  
35  
36  
37  
38  
39  
40  
41  
42  
43  
44  
45  
46  
47  
48  
49  
50  
51  
52  
53  
54  
55  
56  
57  
58  
59  
60



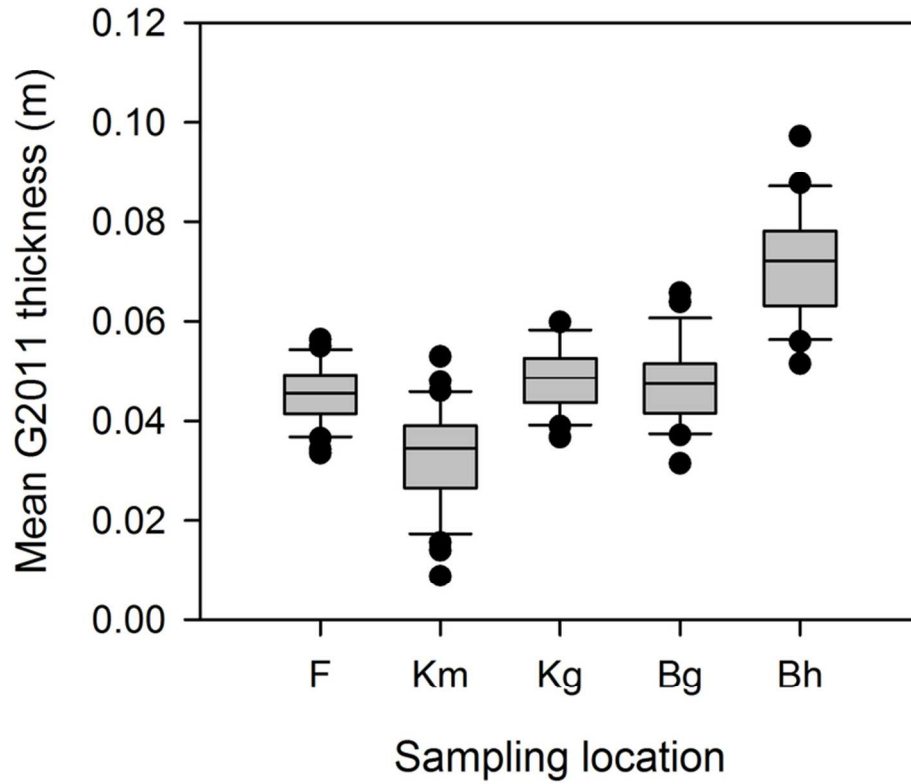
212x315mm (300 x 300 DPI)



135x101mm (300 x 300 DPI)

Review

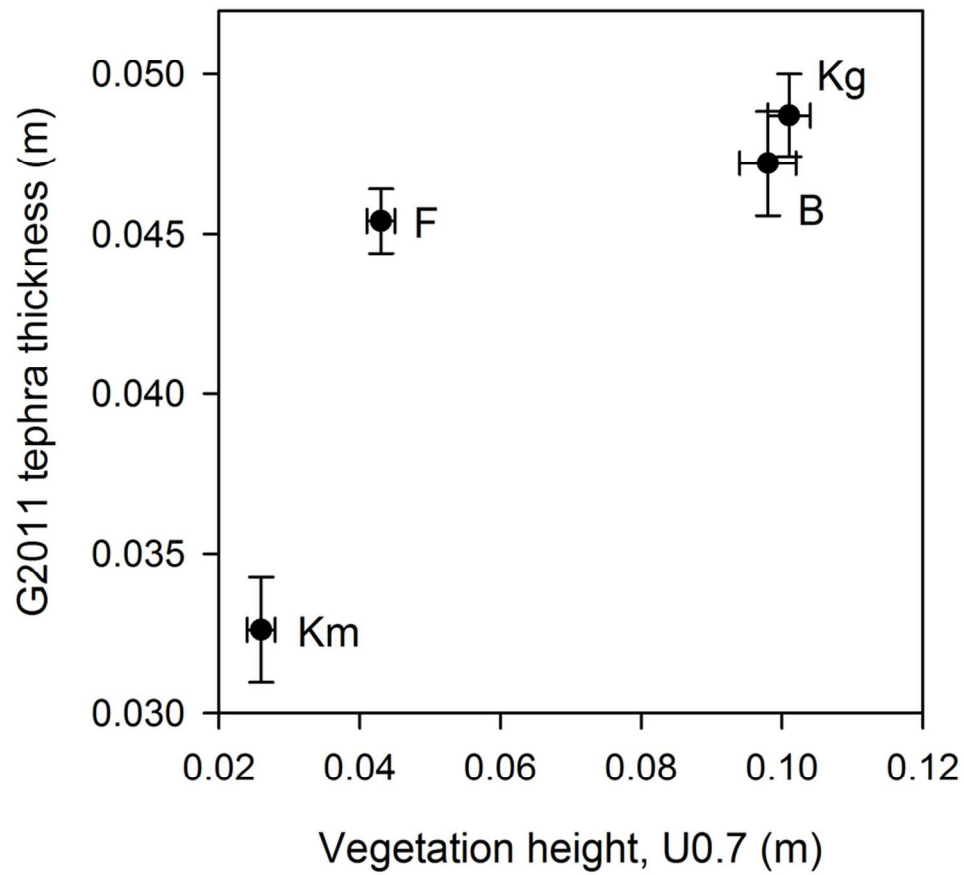
1  
2  
3  
4  
5  
6  
7  
8  
9  
10  
11  
12  
13  
14  
15  
16  
17  
18  
19  
20  
21  
22  
23  
24  
25  
26  
27  
28  
29  
30  
31  
32  
33  
34  
35  
36  
37  
38  
39  
40  
41  
42  
43  
44  
45  
46  
47  
48  
49  
50  
51  
52  
53  
54  
55  
56  
57  
58  
59  
60



76x70mm (300 x 300 DPI)

mc

1  
2  
3  
4  
5  
6  
7  
8  
9  
10  
11  
12  
13  
14  
15  
16  
17  
18  
19  
20  
21  
22  
23  
24  
25  
26  
27  
28  
29  
30  
31  
32  
33  
34  
35  
36  
37  
38  
39  
40  
41  
42  
43  
44  
45  
46  
47  
48  
49  
50  
51  
52  
53  
54  
55  
56  
57  
58  
59  
60



86x88mm (300 x 300 DPI)



1  
2  
3  
4  
5  
6  
7  
8  
9  
10  
11  
12  
13  
14  
15  
16  
17  
18  
19  
20  
21  
22  
23  
24  
25  
26  
27  
28  
29  
30  
31  
32  
33  
34  
35  
36  
37  
38  
39  
40  
41  
42  
43  
44  
45  
46  
47  
48  
49  
50  
51  
52  
53  
54  
55  
56  
57  
58  
59  
60